Am J Physiol Renal Physiol 283: F1200–F1207, 2002.
First published July 30, 2002; 10.1152/ajprenal.00043.2002.

Role of membrane proteins in permeability barrier function: uroplakin ablation elevates urothelial permeability

PING HU,[1] SUSAN MEYERS,[2] FENG-XIA LIANG,[1] FANG-MING DENG,[1] BECHARA KACHAR,[3] MARK L. ZEIDEL,[2] AND TUNG-TIEN SUN[1]

[1]*Ronald O. Perelman Department of Dermatology and Departments of Pharmacology and Urology, Kaplan Comprehensive Cancer Center, New York University School of Medicine, New York, New York 10016;* [2]*Departments of Medicine and Cell Biology and Physiology, University of Pittsburgh School of Medicine, Pittsburgh, Pennsylvania 15213; and* [3]*Laboratory of Cellular Biology, National Institute on Deafness and Other Communication Disorders, National Institutes of Health, Bethesda, Maryland 20892*

Received 31 January 2002; accepted in final form 11 July 2002

Hu, Ping, Susan Meyers, Feng-Xia Liang, Fang-Ming Deng, Bechara Kachar, Mark L. Zeidel, and Tung-Tien Sun. Role of membrane proteins in permeability barrier function: uroplakin ablation elevates urothelial permeability. *Am J Physiol Renal Physiol* 283: F1200–F1207, 2002. First published July 30, 2002; 10.1152/ajprenal.00043.2002.—Although water, small nonelectrolytes, and gases are freely permeable through most biological membranes, apical membranes of certain barrier epithelia exhibit extremely low permeabilities to these substances. The role of integral membrane proteins in this barrier function has been unclear. To study this problem, we have ablated the mouse gene encoding uroplakin III (UPIII), one of the major protein subunits in urothelial apical membranes, and measured the permeabilities of these membranes. Ablation of the UPIII gene greatly diminishes the amounts of uroplakins on the apical urothelial membrane (Hu P, Deng FM, Liang FX, Hu CM, Auerbach AB, Shapiro E, Wu XR, Kachar B, and Sun TT. *J Cell Biol* 151: 961–972, 2000). Our results indicate that normal mouse urothelium exhibits high transepithelial resistance and low urea and water permeabilities. The UPIII-deficient urothelium exhibits a normal transepithelial resistance (normal 2,024 ± 122, knockout 2,322 ± 114 $\Omega \cdot cm^2$; $P > 0.5$). However, the UPIII-deficient apical membrane has a significantly elevated water permeability (normal 0.91 ± 0.06, knockout 1.83 ± 0.14 cm/s $\times 10^{-5}$; $P < 0.05$). The urea permeability of the UPIII-deficient membrane also increased, although to a lesser extent (normal 2.22 ± 0.24, knockout 2.93 ± 0.31 cm/s $\times 10^{-6}$; $P = 0.12$). These results indicate that reduced targeting of uroplakins to the apical membrane does not significantly alter the tight junctional barrier but does double the water permeability. We provide the first demonstration that integral membrane proteins contribute to the apical membrane permeability barrier function of urothelium.

urothelium; uroplakin; permeability; vesicoureteral reflux; knockout

THE MAMMALIAN BLADDER MAINTAINS for prolonged periods large gradients for water, small nonelectrolytes, ions, protons, and ammonium between the urine it stores and blood (4, 5, 16, 36). Thus in humans, urine osmolality varies widely between 50 and 1,000 mosmol/kgH_2O, but blood osmolality remains constant between 280 and 290 mosmol/kgH_2O. Similarly, urinary pH varies from 4.5 to 8.0 while blood pH remains stable at around 7.4 (4, 5, 16, 36). The urothelial barrier function is therefore essential for the kidney to maintain homeostasis. Measurements of barrier function in vitro indeed showed that the bladder exhibits exceptionally low permeabilities to ions (transepithelial resistances of 20,000–30,000 $\Omega \cdot cm^2$) as well as to water and urea (2, 15–18, 21, 25). The apical membranes and the tight junctions between the uppermost urothelial cells (the so-called umbrella cells), in combination, represent the main site of the bladder permeability barrier (15, 17, 18, 21, 25).

The apical membranes of umbrella cells are covered with numerous rigid-looking plaques consisting of two-dimensional hexagonal arrays of 16-nm particles (1, 6, 11, 13, 27, 29, 31). Purified urothelial plaques contain four major integral membrane proteins called uroplakins that are synthesized as the major differentiation products of mammalian urothelia (24, 28, 32–35). Although much has been learned about the sequences of these proteins as well as some aspects of their three-dimensional structure as a complex within the membrane, relatively little is known about their precise function. The hypothesized functions of urothelial plaques include the reversible adjustment of urothelial apical surface (5, 18, 19) and the physical strengthening of the apical surface (27). In addition, because the urothelium represents such an effective barrier, it is tempting to speculate that urothelial plaques augment specialized lipid structures and contribute to bladder barrier function (4, 5). To test these hypotheses, we have developed knockout mice lacking a functional uroplakin III (UPIII) gene (9). These mice not only lack

Address for reprint requests and other correspondence: M. L. Zeidel, Dept. of Medicine, Univ. of Pittsburgh School of Medicine, Rm. 1218 Scaife Hall, 3550 Terrace St., Pittsburgh, PA 15213 (E-mail: Zeidel@msx.dept-med.pitt.edu); or T-T Sun, Depts. of Pharmacology and Urology, New York Univ. Medical School, 550 First Ave., New York, NY 10016 (E-mail: sunt01@mcrcr.med.nyu.edu).

The costs of publication of this article were defrayed in part by the payment of page charges. The article must therefore be hereby marked "*advertisement*" in accordance with 18 U.S.C. Section 1734 solely to indicate this fact.

UPIII but also have a markedly attenuated expression and apical targeting of the other three uroplakins (UPIa, UPIb, and UPII), resulting in a greatly reduced number and average size of the apical plaques. The animals also develop vesicoureteral reflux and hydronephrosis (9).

The present studies focus on the effects of ablating the UPIII gene on the barrier function of the urothelium, in terms of the apical membrane permeabilities and of tight junctional function. We show here that the depletion of uroplakins from urothelial apical surface had no effects on transepithelial resistance but led to elevated water permeability. These results provide the first evidence that integral membrane proteins play a role in establishing certain aspects of urothelial barrier function, possibly by influencing the asymmetry and by reducing the fluidity of the bilayer leaflets.

METHODS

Materials and solutions. Unless specified otherwise, all chemicals were obtained from Sigma (St. Louis, MO) and were of reagent grade. The composition of the NaCl-Ringer bathing solution was (in mM) 111.2 NaCl, 25 $NaHCO_3$, 5.8 KCl, 2 $CaCl_2$, 1.2 $MgSO_4$, 1.2 KH_2PO_4, and 11.1 glucose. This solution was oxygenated with 95% O_2-5% CO_2, pH 7.4, at 37°C.

Mouse strains. The generation and characterization of the UPIII knockout mice were described earlier (9). The knockout vector was designed to delete the first three exons of the UPIII gene. Two 129/SvEv embryonic stem cell (line W4) clones harboring the correct homologous recombination events were amplified, aggregated with eight cell-stage embryos of Swiss Webster (SW) mice, and implanted into pseudopregnant females. Five chimeric mice from these two embryonic stem cell lines were germline transmitting and were bred with SW mice to yield hybrid homozygotes or mated with 129/SvEv mice to yield inbred 129/SvEv UPIII knockout mice (9). The SW mice used as the control and knockout mice were homozygous for UPIII deletion (9). Mice were maintained overnight in metabolic cages for urine collection. All mice had free access to water and a normal mouse chow diet for all experiments.

Measurement of urothelial barrier function. Animal experiments were performed in accordance with the animal use and care committees of both New York University and the University of Pittsburgh. Bladders were excised after lethal anesthesia, washed in oxygenated NaCl Ringer solution, and carefully stretched and mounted on a small ring in the same solution at 37°C. The bladder was then placed between modified Ussing chambers (15, 16, 25). Both compartments of the chambers were under constant stirring and temperature control and allowed electrical measurements and sampling.

The transepithelial potential was measured as described, with Ag-AgCl electrodes placed close to and on opposite sides of the epithelium (15, 16, 25). Transepithelial resistance was determined by passing current through the Ag-AgCl electrodes placed in the rear of each half-chamber across the tissue and measuring the resulting voltage deflection. Both voltage-sensing and current-passing electrodes were connected to an automatic voltage clamp (EC-825, Warner Instruments, Hamden, CT), which was, in turn, connected to a microcomputer with a MacLab interface (16).

All permeability measurements were performed at 37°C after stabilization of the transepithelial resistance. Diffusive water, urea, and butanol permeability coefficients were determined by using isotopic fluxes as described (15, 16, 25). Briefly, tritiated water, [^{14}C]urea or [^{14}C]butanol were added to the apical chamber (13.5-ml total volume) and 100-μl samples of both apical and basolateral chambers were taken every 15 min. Sample volumes were replaced quantitatively with warmed NaCl-Ringer. Sample radioactivities were counted with a liquid scintillation counter (model 1500, Packard Tri-Carb), and flux rates and permeabilities were calculated as described (15, 16, 25). To determine the contribution of unstirred layers to the observed flux rates, water and urea fluxes were measured after the exposure of the bladder apical surface to Triton X-100 (7.4 μl/ml). In some experiments, unstirred layers were measured with [^{14}C]butanol (15). Because these results agreed with those obtained with Triton X-100, the values obtained with Triton X-100 were used to correct for unstirred layer effects. Water and urea permeability are reported as apical membrane permeabilities, in which unstirred layers have been taken into account.

Electron microscopy. For transmission electron microscopy (EM), mouse bladder was cut into small pieces (<1 mm^2), fixed with 2.5% glutaraldehyde in 0.1 M sodium cacodylate buffer, pH 7.4, postfixed with 1% (wt/vol) osmium tetroxide, and embedded in Epon 812 (Polysciences) as described (23). For scanning EM, bladders were bisected, fixed as above, and critical point dried (11).

RESULTS

Effects of UPIII knockout on organ structure and kidney function. Although the UPIII knockout mice appeared healthy, detailed measurements of the body and kidney weights as well as the diameters of the stretched bladder revealed some abnormalities (Table 1). In both males and females, bladders were larger in diameter in UPIII knockout animals compared with controls ($P < 0.001$ for both sexes). In male mice, body and kidney weights of the knockouts were not statistically different from the control animals. However, in female mice, the knockout animals were smaller and their kidneys were larger ($P < 0.05$) than the controls. Pathological examination of kidneys from knockout animals of both sexes showed dilatation of the renal pelvis, as well as clear-cut hydronephrosis, whereas control animals exhibited normal renal morphology (9). Glomeruli appeared normal in knockout and control animals. Bladders from knockout animals were far more easily stretched onto the rings of the Ussing chambers than the bladders from control animals. These results indicate that the lack of UPIII expression made the bladder as a whole more compliant than in control animals.

To assess the kidney functions, we measured the urine chemistry of control and knockout animals (Ta-

Table 1. *Body weight, kidney weight, and bladder size of control and uroplakin III-deficient mice*

Animal Type	*n*	Body Wt, g	Kidney Wt, g	Bladder Diameter, mm
Male control	11	39.8 ± 1.4	0.76 ± 0.04	10.1 ± 0.3
Male knockout	20	38.3 ± 1.1	0.69 ± 0.02	12.9 ± 0.3
Female control	17	36.3 ± 1.5	0.49 ± 0.02	9.1 ± 0.3
Female knockout	12	30.8 ± 0.9	0.60 ± 0.03	12.1 ± 0.5

ble 2). Urinary chloride concentrations were similar in controls and knockout mice, as were creatinine values. Knockout animals exhibited statistically significant higher levels of uric acid and lower levels of potassium and sodium than controls per unit volume of urine ($P < 0.05$). In addition, urinary specific gravity was strikingly reduced in knockout animals compared with controls ($P < 0.001$). The fact that the knockout animals excreted a more dilute urine than control animals suggested a concentrating defect likely due to chronic hydronephrosis and ongoing distal nephron dysfunction (3).

Barrier function of bladders from control and knockout mice. To assess the effects of UPIII depletion on the permeability function of the urothelium, we measured the transepithelial resistance, water permeabilities, and urea permeabilities of control and UPIII knockout mice (Fig. 1). These parameters of normal mouse urothelium were found to be comparable to those of other species, including rats, rabbits, guinea pigs, and cats, thus establishing that the bladders of all of these species exhibit high transepithelial resistances, as well as strikingly low permeabilities to water and urea (Table 3) (2, 4, 15, 16, 19, 21). Although all of the water permeabilities are low, the permeability of the mouse urothelium is four- to fivefold lower than that of the rat or the cat. Figure 1 shows the permeability data for control and knockout mouse bladders, with corrections for unstirred layers. Transepithelial resistances were similar between control and knockout animals, suggesting that the ablation of UPIII did not alter the function of the tight junctions between umbrella cells. By contrast, water permeability was clearly increased in bladders from knockout animals compared with controls ($P < 0.05$). Urea permeability tended to be higher in the knockout animals as well, although this apparent difference did not reach statistical significance ($P = 0.12$). When data from males and females were pooled, urea permeability was significantly higher in the UPIII knockout mice than in controls ($P \leq 0.05$). For resistance, water, and urea permeabilities, values for control or knockout mice did not differ between male and female mice. In all cases, addition of Triton X-100 increased the measured fluxes of water and urea by more than fourfold; these increases were similar in control and knockout animals. These results indicate that the unstirred layers were similar in magnitude for the control and knockout bladders and that the observed differences in the permeability of normal and UPIII knockout animals could be attributed to differences in the properties of the apical membrane.

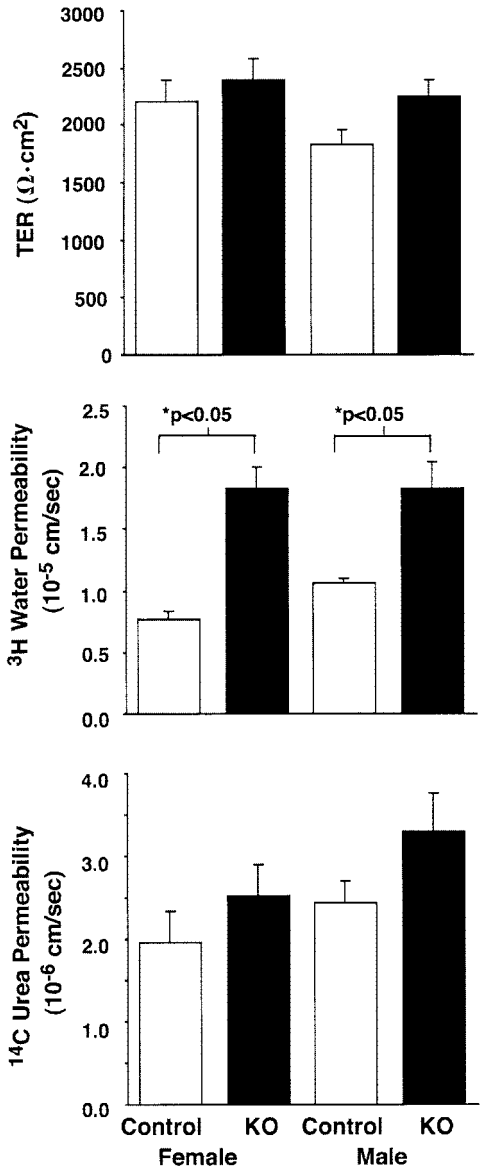

Fig. 1. Transepithelial resistances (TER; *top*), apical membrane water permeabilities (*middle*), and apical membrane urea permeabilities (*bottom*) of bladders from male and female control and uroplakin III (UPIII) knockout (KO) mice. Note that the apical membrane water permeabilities were significantly higher in the UPIII knockout mice than in control animals.

Table 2. *Urine chemistry of control and uroplakin III knockout mice*

Measurement	*n*	All Controls	All Knockouts
Creatinine	10	38.6 ± 3.1	39.3 ± 3.0
Sodium	10	97.2 ± 9.3	75.7 ± 5.8
Potassium	10	209.3 ± 9.7	184.1 ± 8.0
Chloride	10	144.6 ± 10.3	116.1 ± 8.8
Uric acid	10	6.3 ± 0.4	9.4 ± 0.7
Specific gravity	20	1.067 ± 0.004	1.040 ± 0.002

Spontaneous transepithelial voltages across bladders from control mice averaged 5.2 ± 0.9 mV (lumen negative), whereas those across knockout mice averaged 3.8 ± 0.8 mV (n = 21–27 for each group). There was no significant difference between males and females and between control and knockout mice. Short-circuit current, which estimates the rate of ion transport across the epithelium, averaged 1.8 ± 0.2 μA/μF in bladders from control animals and 1.7 ± 0.3 μA/μF in bladders from knockout mice (n = 21–27 for each group). There was no significant difference between male and female mice or between control and knockout

Table 3. *Urothelial permeabilities of species*

Species	Transepithelial Resistance, $\Omega \cdot cm^2$	Water Permeability, cm/s $\times 10^{-5}$	Urea Permeability, cm/s $\times 10^{-6}$
Mice	2,200 ± 190	0.8 ± 0.1	2.0 ± 0.4
Rabbits	3,210 ± 800	5.2 ± 0.4	4.5 ± 0.7
Guinea pigs	2,380 ± 290	5.7 ± 0.7	1.7 ± 0.1
Rats	1,770 ± 210	2.7 ± 0.2	1.4 ± 0.2
Cats	3,300 ± 560	4.0 ± 0.8	1.5 ± 0.3

Water and urea permeability values are corrected for unstirred layer effects by permeabilizing the apical membrane with Triton X-100. These values therefore represent apical membrane permeabilities (15, 15a, 16, 24).

mice. The short-circuit current values are at the lower range of those observed in isolated rabbit urothelia by Lewis and Diamond (20). This could be because all animals in our experiments had free access to salt, showed urinary potassium-to-sodium ratios in the range of 2.1:2.4, and likely maintained low levels of aldosterone (20).

Water flux across water channels has an activation energy <5 kcal·mol^{-1}·K^{-1} whereas that across membranes that lack water channels is >10 kcal·mol^{-1}·K^{-1} (7, 8, 14, 36). Because the water permeability was increased in the bladders from knockout animals, it was possible that an aquaporin was being expressed in the apical membranes of the knockout animals. We therefore measured the rate of water flux in individual bladders from control and knockout mice at three different temperatures between 28 and 40°C. The activation energies ranged from 11.5 to 12.5 kcal·mol^{-1}·K^{-1} in control and knockout animals alike. These results indicate that the increased rate of water flux in knockout animals was not due to flux via water channels.

EM of bladders from control and knockout mice. To determine the ultrastructural bases for the observed physiological alterations, we examined the umbrella cells from control and knockout animals by transmission (Fig. 2) and scanning EM (Fig. 3), paying special attention to cell/cell junctions. Umbrella cells from control animals exhibited numerous fusiform subapical vesicles and an apical surface that was covered with plaques; in contrast, the superficial cells from knockout animals had small, round immature vesicles and few apical surface plaques (Fig. 2 and see also Ref. 9). Umbrella cells from both control and knockout animals had well-developed tight junctions (Fig. 2). However, in knockout animals there appeared to be an increase in the number of desmosomes, a feature that was observed in numerous fields in tissues taken from multiple bladders from both control and knockout animals (Fig. 2). Scanning EM of umbrella cells from normal mouse urothelium revealed large cells covered by ridges (most likely due to the presence of numerous urothelial plaques) on their apical surfaces (Fig. 3) (5, 9, 10, 16, 26). In contrast, surface cells in knockout animals displayed numerous microvilli, and the cells were far smaller than those of bladders from control animals (Fig. 3 and see also Ref. 9).

DISCUSSION

Uroplakin knockout increases the water permeability of urothelial membrane. We showed here that the ablation of UPIII doubled the water permeability of urothelial membrane. Because the absolute value for water permeability of the bladders from knockout animals was still quite low, it is important to rule out the possibility of an "unstirred layer" effect, whereby the unstirred layer adjacent to the urothelial apical surface limits the extent to which an increased rate of water flux could be detected in our apparatus. However, addition of Triton X-100 to the apical surface of the urothelium from both control and knockout mice led to similar striking increases in water permeability. This proves that had water permeability in knockout animals been higher, we would have been able to detect it, and the loss of UPIII results in only a partial reduction in the water barrier function (see below).

The strikingly low water permeabilities of both control and UPIII knockout urothelia suggest that the lipid component of the mouse urothelial apical membrane is particularly resistant to water permeation and that this resistance persists even when the levels of uroplakins in the apical membrane are markedly reduced. Future studies will address the lipid structures of the apical membranes in control and uroplakin knockout mice. An additional issue concerns the surface area of apical membrane in control and knockout animals. Although the surface area of epithelium was identical in the two preparations, we cannot quantify the levels of surface area of membrane in situ in the two animal types because we cannot measure capacitance in the intact bladder.

Complementary roles of lipids and integral membrane proteins in barrier function. In prior studies of barrier apical membranes, we and others have determined the unique lipid compositions of urothelial plaques (12, 30) and defined certain aspects of lipid structure that play a critical role in reducing the membrane permeabilities to small molecules (7, 8, 14, 25). Biological membranes have asymmetric lipid bilayers, with phosphatidyl choline, glycosphingolipids (such as cerebrosides), sphingomyelin, and cholesterol segregated in the outer leaflet, and phosphatidyl serine and ethanolamine segregated in the inner or cytoplasmic leaflet (7, 8, 14, 25). Because the outer and inner leaflets of the bilayer act as independent resistors of permeation (8), barrier membranes tend to use phospholipids whose fatty acids have few double bonds and to have large quantities of sphingomyelin and cholesterol (which rigidify the acyl chains of the fatty acids) in their outer leaflets (7, 8, 14, 25). It is entirely possible that the special composition and structural packing of lipids that are characteristic of the urothelial apical membrane are largely responsible for the extraordinarily effective urothelial barrier function. However, how the lipids accomplish this task and whether membrane proteins also play a role in this process remain unclear.

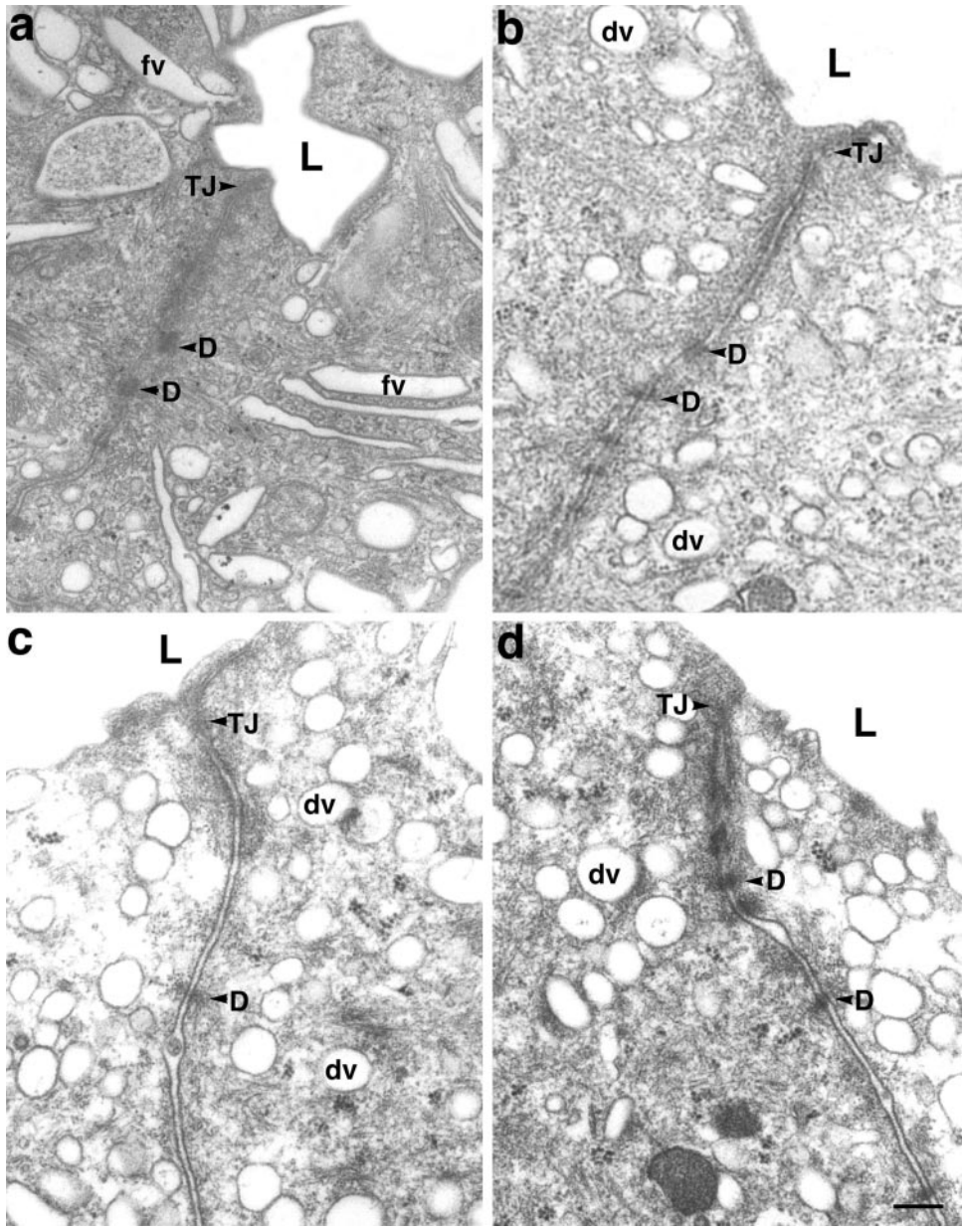

Fig. 2. Cellular junctions between superficial umbrella cells of normal (*a*) and UPIII-deficient mouse urothelia (*b–d*). Note, in normal urothelium, the plaque-lined apical surface, facing the lumen (L), abundant cytoplasmic fusiform vesicles (fv), and apical junctional complex consisting of tight junctions (TJ) and desmosomes (D); also note, in UPIII-deficient urothelium, the lack of apical surface plaques, the replacement of fusiform vesicles by immature discoidal vesicles (DV), the presence of normal-looking tight junctions, and the greatly increased number of desmosomes. Bar = 200 nm.

A striking feature of mammalian urothelial apical membrane is that >90% of this membrane is covered by two-dimensional crystalline arrays of 16-nm protein particles (6, 13, 27, 29). These plaques are composed of four major uroplakins, i.e., UPIa (27 kDa), UPIb (28 kDa), UPII (15 kDa), and UPIII (47 kDa) (28). The fact that most of the hydrophilic domains of uroplakins are extracellular can account for the fact that the outer leaflet of apical urothelial plaques is twice as thick as the inner leaflet (24, 28, 33, 34). These crystalline arrays of uroplakins form rigid-appearing plaques within the apical membrane; areas between the plaques are referred to as hinge regions (22). We showed recently that the ablation of UPIII gene results in a marked diminution of the plaque surface area in favor of hinge regions and that UPIII knockout led to vesicoureteral reflux (9). UPIII knockout mice thus provide an excellent model for defining the role of uroplakins in urothelial physiology and have allowed us to establish in this study a role of uroplakin proteins in water barrier function (Fig. 1).

Possible mechanism of uroplakin influence on barrier function. There are several possible mechanisms by which uroplakins affect the water permeability of urothelium. Thus uroplakins may function by organizing and rigidifying the lipids in the outer leaflet of the bilayer so that water cannot penetrate into the aliphatic chains of the fatty acids (7, 8). Alternatively, uroplakins may stabilize a particularly rigid set of lipids within the outer leaflet. These mechanisms seem reasonable given our earlier finding that the 16-nm urothelial particle is a mushroom-shaped structure with a 16-nm head domain that is exposed luminally and is anchored into the lipid bilayer via a thinner

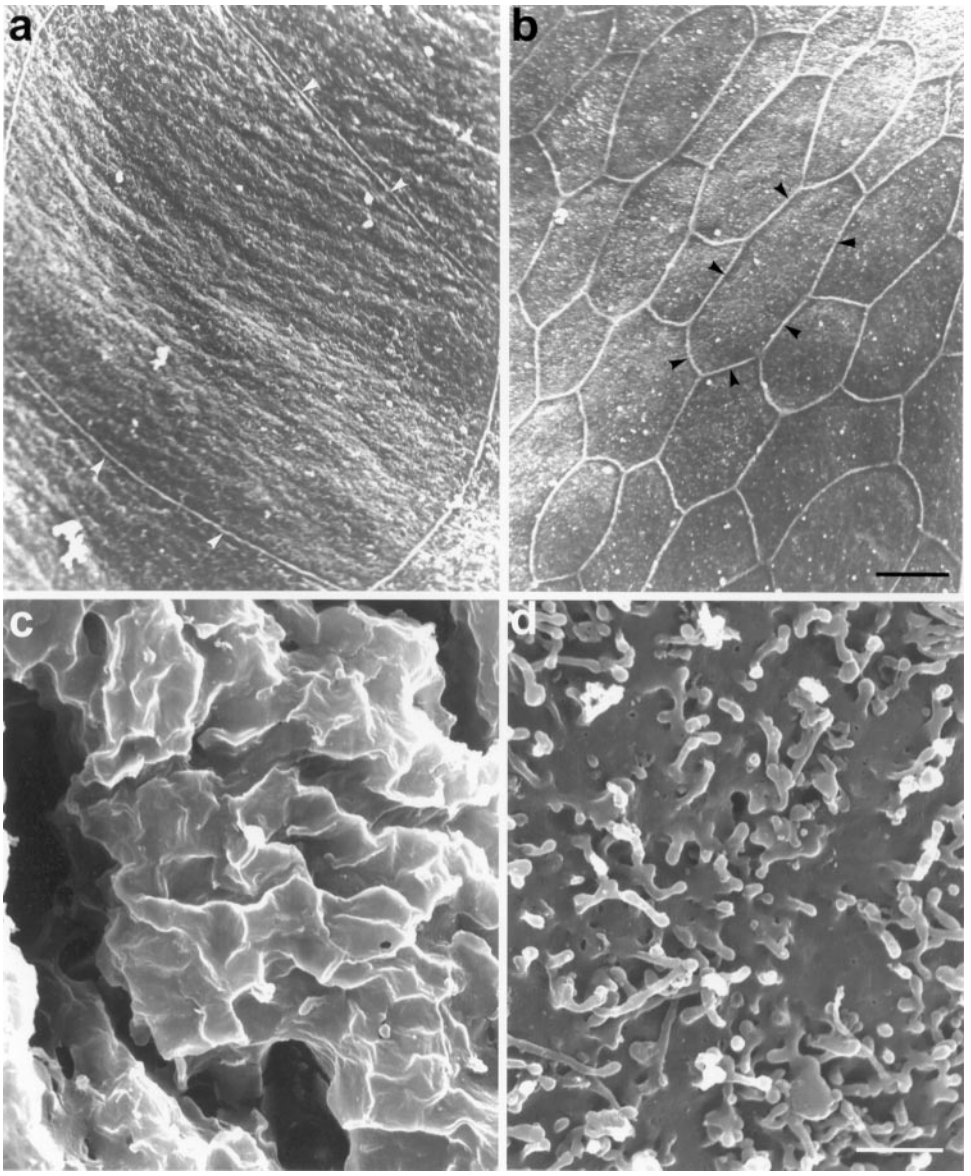

Fig. 3. Apical cell surface morphology of normal (*a* and *c*) and UPIII-deficient (*b* and *d*) mouse urothelia as seen by scanning electron microscopy. Note the greatly reduced apical cell size in the UPIII knockout mouse urothelium (*b*) compared with normal (*a*). Arrowheads, cell boundaries. Also note the replacement of the normal rugged apical cell morphology (*c*) by microvilli in the UPIII-deficient urothelium (*d*). Bars = *a* and *b*, 10 μm; *c* and *d*, 2.5 μm.

11-nm transmembrane domain (11). The transmembrane domains of uroplakins are most likely also regularly packed forming two-dimensional crystalline structures that can exert major constraints on the arrangement of lipid molecules. In addition, the uroplakin domains that are close to the outer and inner leaflet of the bilayer are clearly asymmetrical (34); this protein asymmetry may exert strong constraints on the allowable lipid composition of the outer and inner leaflets. The uroplakin proteins may therefore play a major role in determining both the asymmetrical lipid composition of the two leaflets and the rigidity of the (interparticle) lipid components, thereby influencing the overall permeability of the apical urothelial membrane. The fact that the apical urothelial surface of UPIII knockout mice is still partially covered by urothelial plaques, albeit smaller (9), may explain why the water barrier function was only partially compromised.

Other functional roles of uroplakins. The ablation of the UPIII gene had several striking effects on cell structure (9). Umbrella cells from knockout animals lacked apical membrane plaques on transmission EM (Fig. 2) and exhibited microvilli rather than ridges on scanning EM (Fig. 3). Their subapical vesicles were discoidal rather than fusiform (Fig. 2). In addition, the cells were smaller than in control animals (Fig. 3), and it appeared that the junctions between the cells had more desmosomes in knockout animals (Fig. 2). These results indicate that uroplakins are responsible for the unique shape of the apical membranes and of the subapical vesicles of umbrella cells.

It is unclear why cells lacking uroplakin do not grow to the large size of normal umbrella cells. It is possible that the absence of uroplakin renders the apical membrane unstable as it expands so that umbrella cells that become too large disintegrate and are sloughed off. This interpretation is consistent with our laborato-

ry's recent observation that there seem to be more apoptotic cells than control cells detaching from the UPIII-deficient urothelium (9). In unpublished studies in which we have induced a selective injury to the umbrella cells by using protamine, we have shown that regenerating urothelial cells reach the surface and develop normal ridges, normal plaques, and normal barrier function before they begin to enlarge (Lavelle JP, Meyers S, Doty D, Apodaca G, and Zeidel ML, unpublished observations).

Uroplakin knockout does not affect the tight junctional function. An unexpected finding was that UPIII knockout mice had no apparent effects on transepithelial resistance, and EM revealed that knockout animals exhibited intact tight junctions. These results indicate that uroplakins play no role in the formation of tight junctions and that the lack of uroplakins does not appear to alter trafficking of essential tight junctional proteins such as claudins to the correct location (Fig. 2). Because the surface urothelial cells are smaller in the knockout animals, tight junctions actually occupy a much higher proportion of the apical surface area in these animals than in controls. Because these studies were performed in intact bladders rather than dissected urothelium, our measured transepithelial resistances for bladders from both control and knockout mice were well below the 20,000 $\Omega \cdot cm^2$ that is observed with dissected urothelium. This prevented us from determining whether the tight junctions in the knockout animals functioned quantitatively as well as those of the controls. It is also unclear why there appear to be more desmosomes in the knockout animals than in the controls.

In summary, we demonstrate here that UPIII deficiency had no effects on transepithelial resistance, indicating that the tight junctional aspect of the urothelial barrier remained intact and that the water permeability barrier was compromised, indicating that uroplakins play a key role in establishing the permeability barrier for water and possibly some other polar substances. Our data provide the first indication that an integral membrane protein, most likely in conjunction with specific lipid components, can participate in reducing the permeabilities in a barrier epithelium.

We thank Alexander Joyner for advice on the generation of the knockout mice and Edith S. Robbins and David Sabatini for use of their electron microscopes.

This work was supported by National Institute of Diabetes and Digestive and Kidney Diseases Grants DK-43955 and DK-48217 (to M. L. Zeidel) and DK-52206, DK-57269, and DK-3975 (to T.-T. Sun).

REFERENCES

1. **Brisson A and Wade RH.** Three-dimensional structure of luminal plasma membrane protein from urinary bladder. *J Mol Biol* 166: 21–36, 1983.
2. **Chang A, Hammond TG, Sun TT, and Zeidel ML.** Permeability properties of the mammalian bladder apical membrane. *Am J Physiol Cell Physiol* 267: C1483–C1492, 1994.
3. **Curhan GC, McDougal WS, and Zeidel ML.** Urinary tract obstruction. In: *The Kidney*, edited by Brenner BM. Philadelphia: Saunders, 2000.
4. **Hicks RM.** The permeability of rat transitional epithelium. Keratinization and the barrier to water. *J Cell Biol* 28: 21–31, 1966.
5. **Hicks RM.** The mammalian urinary bladder: an accommodating organ. *Biol Rev Camb Philos Soc* 50: 215–246, 1975.
6. **Hicks RM and Ketterer B.** Hexagonal lattice of subunits in the thick luminal membrane of the rat urinary bladder. *Nature* 224: 1304–1305, 1969.
7. **Hill WG, Rivers RL, and Zeidel ML.** Role of leaflet asymmetry in the permeability of model biological membranes to protons, solutes, and gases. *J Gen Physiol* 114: 405–414, 1999.
8. **Hill WG and Zeidel ML.** Reconstituting the barrier properties of a water-tight epithelial membrane by design of leaflet-specific liposomes. *J Biol Chem* 275: 30176–30185, 2000.
9. **Hu P, Deng FM, Liang FX, Hu CM, Auerbach AB, Shapiro E, Wu XR, Kachar B, and Sun TT.** Ablation of uroplakin III gene results in small urothelial plaques, urothelial leakage, and vesicoureteral reflux. *J Cell Biol* 151: 961–972, 2000.
10. **Jacobs JB, Arai M, Cohen SM, and Friedell GH.** Early lesions in experimental bladder cancer: scanning electron microscopy of cell surface markers. *Cancer Res* 36: 2512–2517, 1976.
11. **Kachar B, Liang F, Lins U, Ding M, Wu XR, Stoffler D, Aebi U, and Sun TT.** Three-dimensional analysis of the 16 nm urothelial plaque particle: luminal surface exposure, preferential head-to-head interaction, and hinge formation. *J Mol Biol* 285: 595–608, 1999.
12. **Ketterer B, Hicks RM, Christodoulides L, and Beale D.** Studies of the chemistry of the luminal plasma membrane of rat bladder epithelial cells. *Biochim Biophys Acta* 311: 180–190, 1973.
13. **Koss LG.** The asymmetric unit membranes of the epithelium of the urinary bladder of the rat. An electron microscopic study of a mechanism of epithelial maturation and function. *Lab Invest* 21: 154–168, 1969.
14. **Lande MB, Donovan JM, and Zeidel ML.** The relationship between membrane fluidity and permeabilities to water, solutes, ammonia, and protons. *J Gen Physiol* 106: 67–84, 1995.
15. **Lavelle JP, Apodaca G, Meyers SA, Ruiz WG, and Zeidel ML.** Disruption of guinea pig urinary bladder permeability barrier in noninfectious cystitis. *Am J Physiol Renal Physiol* 274: F205–F214, 1998.

15a. **Lavelle J, Meyers S, Ramage R, Bastacky S, Doty D, Apodaca G, and Zeidel ML.** Bladder permeability barrier: recovery from selective injury of surface epithelial cells. *Am J Physiol Renal Physiol* 283: F242–F253, 2002.

16. **Lavelle JP, Meyers SA, Ruiz WG, Buffington CA, Zeidel ML, and Apodaca G.** Urothelial pathophysiological changes in feline interstitial cystitis: a human model. *Am J Physiol Renal Physiol* 278: F540–F553, 2000.
17. **Lewis SA, Berg JR, and Kleine TJ.** Modulation of epithelial permeability by extracellular macromolecules. *Physiol Rev* 75: 561–589, 1995.
18. **Lewis SA and de Moura JL.** Incorporation of cytoplasmic vesicles into apical membrane of mammalian urinary bladder epithelium. *Nature* 297: 685–688, 1982.
19. **Lewis SA and de Moura JL.** Apical membrane area of rabbit urinary bladder increases by fusion of intracellular vesicles: an electrophysiological study. *J Membr Biol* 82: 123–136, 1984.
20. **Lewis SA and Diamond JM.** Na^+ transport by rabbit urinary bladder, a tight epithelium. *J Membr Biol* 28: 1–40, 1976.
21. **Lewis SA and Hanrahan JW.** Physiological approaches for studying mammalian urinary bladder epithelium. *Methods Enzymol* 192: 632–650, 1990.
22. **Liang F, Kachar B, Ding M, Zhai Z, Wu XR, and Sun TT.** Urothelial hinge as a highly specialized membrane: detergent-insolubility, urohingin association, and in vitro formation. *Differentiation* 65: 59–69, 1999.
23. **Liang FX, Riedel I, Deng FM, Zhou G, Xu C, Wu XR, Kong XP, Moll R, and Sun TT.** Organization of uroplakin subunits: transmembrane topology, pair formation and plaque composition. *Biochem J* 355: 13–18, 2001.
24. **Lin JH, Wu XR, Kreibich G, and Sun TT.** Precursor sequence, processing, and urothelium-specific expression of a major 15-

kDa protein subunit of asymmetric unit membrane. *J Biol Chem* 269: 1775–1784, 1994.
25. **Negrete HO, Lavelle JP, Berg J, Lewis SA, and Zeidel ML.** Permeability properties of the intact mammalian bladder epithelium. *Am J Physiol Renal Fluid Electrolyte Physiol* 271: F886–F894, 1996.
26. **Pauli BU, Alroy J, and Weinstein RS.** The ultrastructure and pathobiology of urinary bladder cancer. In: *The Pathology of Bladder Cancer*, edited by Bryan GT and Cohen SM. Boca Raton, FL: CRC, 1983, p. 42–140.
27. **Staehelin LA, Chlapowski FJ, and Bonneville MA.** Lumenal plasma membrane of the urinary bladder. I. Three-dimensional reconstruction from freeze-etch images. *J Cell Biol* 53: 73–91, 1972.
28. **Sun TT, Zhao H, Provet J, Aebi U, and Wu XR.** Formation of asymmetric unit membrane during urothelial differentiation. *Mol Biol Rep* 23: 3–11, 1996.
29. **Vergara J, Longley W, and Robertson JD.** A hexagonal arrangement of subunits in membrane of mouse urinary bladder. *J Mol Biol* 46: 593–596, 1969.
30. **Vergara J, Zambrano F, Robertson JD, and Elrod H.** Isolation and characterization of luminal membranes from urinary bladder. *J Cell Biol* 61: 83–94, 1974.
31. **Walz T, Haner M, Wu XR, Henn C, Engel A, Sun TT, and Aebi U.** Towards the molecular architecture of the asymmetric unit membrane of the mammalian urinary bladder epithelium: a closed "twisted ribbon" structure. *J Mol Biol* 248: 887–900, 1995.
32. **Wu XR, Manabe M, Yu J, and Sun TT.** Large scale purification and immunolocalization of bovine uroplakins I, II, and III. Molecular markers of urothelial differentiation. *J Biol Chem* 265: 19170–19179, 1990.
33. **Wu XR and Sun TT.** Molecular cloning of a 47 kDa tissue-specific and differentiation-dependent urothelial cell surface glycoprotein. *J Cell Sci* 106: 31–43, 1993.
34. **Yu J, Lin JH, Wu XR, and Sun TT.** Uroplakins Ia and Ib, two major differentiation products of bladder epithelium, belong to a family of four transmembrane domain (4TM) proteins. *J Cell Biol* 125: 171–182, 1994.
35. **Yu J, Manabe M, Wu XR, Xu C, Surya B, and Sun TT.** Uroplakin I: a 27-kD protein associated with the asymmetric unit membrane of mammalian urothelium. *J Cell Biol* 111: 1207–1216, 1990.
36. **Zeidel ML.** Low permeabilities of apical membranes of barrier epithelia: what makes watertight membranes watertight? *Am J Physiol Renal Fluid Electrolyte Physiol* 271: F243–F245, 1996.